Surface-Induced Transitions in Thin Films of Asymmetric Diblock Copolymers

H. P. Huinink*

Department of Applied Physics, Eindhoven University of Technology, P.O. Box 513, 5600 MB Eindhoven, The Netherlands

M. A. van Dijk

Shell Research and Technology Centre Amsterdam, Badhuisweg 3, 1031 CM Amsterdam, The Netherlands

J. C. M. Brokken-Zijp

Department of Chemical Engineering, Eindhoven University of Technology, P.O. Box 513, 5600 MB Eindhoven, The Netherlands

G. J. A. Sevink

Leiden Institute of Chemistry, Gorlaeus Laboratories, Leiden University, Einsteinweg 55, P.O. Box 9502, 2300 RA Leiden, The Netherlands

Received January 4, 2000; Revised Manuscript Received April 18, 2001

ABSTRACT: A dynamic density functional theory for polymeric systems has been used to investigate the influence of surface fields on the morphology of thin films of asymmetric diblock copolymers, which form cylinders in a bulk system. We have found that noncylindrical structures become stable when one of the blocks is strongly attracted by the surfaces. When the interaction between the surface and the polymer was increased, two transitions occur: (a) from parallel oriented cylinders to parallel oriented perforated lamellae ($C_{||} \rightarrow CL_{||}$) and (b) from this perforated lamellae to lamellae ($CL_{||} \rightarrow L_{||}$). It has also been observed that the microstructure becomes much more sensitive to the film thickness in the case where the surfaces strongly attract one of the polymer blocks. The influence of the surfaces seems to be limited to a region with a size of the order of one domain−domain distance.

I. Introduction

In the past decade, block copolymer thin films have held considerable attention. Block copolymer films form nanoscale patterns, which could be useful for miniaturization of electronic circuits. From scientific point of view, these films are interesting because a wealth of confinement phenomena can be studied experimentally with relative ease. Thin films of symmetric diblock copolymers, $f \equiv N_A/(N_A + N_B) \approx 0.5$, have been studied in great detail by experimentalists and theoreticians.[1,2] Although, a number of studies on films of asymmetric diblock copolymers have been published,[3−8] systematic knowledge is limited.

Recently, we have proposed a phase diagram for an asymmetric diblock copolymer ($f = 0.33$) confined in a slit, by using a dynamic density functional theory (DDFT) for polymeric systems.[5] It was found that the behavior of cylinder-forming asymmetric diblock copolymers bears many similarities to the behavior of symmetric diblock copolymers, except that the asymmetric ones formed a cylindrical structure instead of lamellar one. We found that, dependent on the slit width and the polymer−surface interactions, the cylinders either oriented parallel ($C_{||}$) with or perpendicular ($C_{\perp}$) to the surfaces. As in the case of symmetric block copolymers, the orientation of the domains seems to be determined by the balance of two "forces". Selective interactions between the slit surfaces and the polymer blocks tend to align the domains parallel. However, in a parallel morphology the domain−domain distance will deviate from its bulk value, and the polymer chains are somewhat stretched or compressed compared to their bulk conformation. Therefore, the chain entropy favors perpendicular oriented domains.

Beside resemblances between the slit behavior of symmetric and asymmetric block copolymers, we also found differences. Because of symmetry considerations, in slits of symmetric diblock copolymers the confinement and the wetting properties influence only the orientation of the domains but not its shape. In the case of asymmetric block copolymers, even shape transitions can occur. We have found noncylindrical structures like cartenoid−lamellae ($CL_{||}$) and lamellae ($L_{||}$). Surface fields tend to suppress density variations in the direction parallel to the surfaces and therefore stabilize noncylindrical morphologies.

In this paper, we want to study in more detail the influence of confinement and surface fields on the stabilization of noncylindrical morphologies. It has already been shown with a WSL (weak segregation limit) approach that surface fields are able to induce transitions from cylinders to lamellae in a region close to the surfaces.[3] Due to the fact that density variations were allowed in only two dimensions, more complex morphologies like the $CL_{||}$ were not predicted. In this paper we want to investigate systematically the influence of the surface fields (i.e., wetting properties of the

* To whom correspondence should be addressed (e-mail: h.p.huinink@tue.nl).

10.1021/ma000015h CCC: $20.00
Published on Web 06/21/2001

polymer blocks) on the film morphology of asymmetric diblock copolymers, forming a cylindrical phase in the bulk. We want to answer the following questions by performing a systematic model study: Is there one single transition from cylinders to lamellae or does the film structure go through a sequence of phases (like $CL_{||}$) when the attraction between the film surfaces and one of the polymer blocks is increased? What is the influence of confinement on noncylindrical structures? How far does the influence of a surface into the polymer melt reach?

To answer these questions we have used a mean field dynamic density functional theory (DDFT) for polymeric systems. The basic ingredients of the DDFT model are a free energy functional based on the Gaussian chain model and the Langevin equation for diffusive evolution of density fields. The molecular model is a chain of beads connected by Gaussian springs, mimicking the random walk behavior of the polymer. Because of the Langevin equation, the free energy is minimized and the system moves toward a global or sometimes a local minimum.

This model has already been used to study the microphase separation process in block copolymer melts,[9] the phase behavior of water/pluronic mixtures,[10] and shearing effects on the morphology on block copolymer systems.[11] Recently, so-called mask fields have been introduced in the DDFT model, to be able to predict the influence of hard objects on the morphology of block copolymer melts.[12] Our previous study[5] was an application of this DDFT model on a confined film: a polymeric melt confined between two hard walls (a slit). We have argued that these finding can be extrapolated to free films. Recently, also the phase behavior of an aqueous pluronic film has also been studied.[13]

To keep the amount of variables as low as possible, we use exactly the same molecular model as before:[5] A_3B_6 with $\chi N \approx 18$. The bulk behavior of this block copolymer is comparable with an SB (polystyrene−polybutadiene) block copolymer system with $M_w \approx 35\,000$ g/mol at $T \approx 413$ K. We have shown that the model system A_3B_6 forms hexagonally packed A-rich cylinders in a B-rich matrix in a bulk system. As already mentioned, the polymer film is represented as melt confined in a slit with a width H. Only two quantities are varied: the width of slit H and the effective interaction ξ (by definition equal to the scaled difference in A−surface and B−surface interactions).

In the Theory section, we will shortly discuss a few aspects of the DDFT model, which are relevant for our discussion. The results section is divided into three subsections, addressing the different issues we want to investigate. First, the influence of the wetting properties on the film structure is discussed. Second, we will study the influence of confinement on the various predicted morphologies. Third, we will investigate how far the influence of the surfaces on the film morphology reaches.

II. Method

In this section, we briefly review the important theoretical aspects of the DDFT model. For a detailed discussion, we refer the reader to the literature.[9,12,14] The core of the model consists of two ingredients: a free energy functional for polymeric systems and a Langevin equation for diffusion. Because of the dynamic part, the polymer melt will move toward a local or global minimum. In fact, the Langevin equation acts as a minimization procedure.

A. Free Energy. The free energy functional is based on the following microscopic model. A box with periodic boundaries is filled with beads of different types I. The polymer is represented as a chain of beads, connected by Gaussian springs, with a spring constant of $3kT/2a^2$. As a consequence, a single polymer behaves as a random-walk chain. The free energy functional is given by

$$F[\{\rho\}] = -kT \ln\left(\frac{\Phi^n}{n!}\right) - \sum_I \int_V U_I(\vec{r})\rho_I(\vec{r})\, \mathrm{d}\vec{r} + \frac{1}{2}\sum_{I,J}\int_V\int_V \epsilon_{IJ}(\vec{r}-\vec{r}')\rho_I(\vec{r})\rho_J(\vec{r}')\, \mathrm{d}\vec{r}'\, \mathrm{d}\vec{r} + \frac{1}{2}\sum_I \int_V\int_V \epsilon_{IM}(\vec{r}-\vec{r}')\rho_I(\vec{r})\rho_M(\vec{r}')\, \mathrm{d}\vec{r}'\, \mathrm{d}\vec{r} + \frac{1}{2}\kappa_H v^2 \int_V \Big(\sum_I \rho_I(\vec{r}) - \sum_I \bar{\rho}_I\Big)^2 \mathrm{d}\vec{r} \quad (1)$$

where v is the excluded volume of a bead and V is the system volume. Note that the excluded volumes of all bead types are chosen equally. The first two terms on the rhs account for the entropy of system n ideal chains embedded in a self-consistent field $U_I(\vec{r})$, which is conjugate with the density field $\rho_I(\vec{r})$.

The third term on the rhs is the energy due to bead−bead interactions. The bead−bead interaction potential $\epsilon_{IJ}(\vec{r}-\vec{r}')$ describes the interactions between the beads I and J at the positions $\vec{r}$ and $\vec{r}'$. Gaussian kernels are used for these potentials:

$$\epsilon_{IJ}(\vec{r}-\vec{r}') \equiv \epsilon^\circ_{IJ}\left(\frac{3}{2\pi a^2}\right)^{3/2} \exp\left[-\frac{3}{2a^2}(\vec{r}-\vec{r}')^2\right] \quad (2)$$

From eq 2, it follows that the range of the interactions is comparable to the size of the chain fragments represented by the beads. The parameter ϵ°_{IJ} is related to the Flory−Huggins parameter, $\chi_{IJ} = (\epsilon^\circ_{IJ} + \epsilon^\circ_{JI} - \epsilon^\circ_{II} - \epsilon^\circ_{JJ})/2vkT$, and can be interpreted as a cohesive energy. The functional form of the potential captures the most important physics and is easy to handle.

The fourth term of eq 1 accounts for interactions between the beads and the slit surfaces. The potential $\epsilon_{IM}(\vec{r}-\vec{r}')$ has the same functional dependence as the bead−bead interaction potential (eq 2). In the DDFT model the density field $\rho_M(\vec{r})$ is used to describe inert objects (masks); $\phi_M \equiv \rho_M v = 1$ inside and $\phi_M = 0$ outside the objects. The last term of eq 1 models the excluded volume interactions. A free energy penalty is imposed when locally the total density deviates from its average value. The parameter K_H is the Helfand compressibility parameter.

B. Dynamics. As already has been said, the evolution of density fields is predicted by using the Langevin equation for diffusion. In fact, this equation minimizes the free energy with respect to the density fields $\{\rho_I(\vec{r})\}$. This equation is given by

$$\frac{\partial \rho_I}{\partial t} = M_I \nabla\cdot\rho_I \nabla\mu_I + \eta_I \quad (3)$$

where $\mu_I = \delta F/\delta\rho_I$ is the intrinsic chemical potential, M_I is the mobility and η_I is noise, which is Gaussian-distributed with moments dictated by the fluctuation dissipation theorem. In the neighborhood of hard objects, rigid wall boundary conditions are used. These conditions are implemented by using

$$\vec{n}\cdot\Delta\mu_I = 0 \quad (4)$$

where $\vec{n}$ is the normal pointing toward the object. The same boundary conditions are used for the noise η_I.

C. Computational Procedure. The free energy of the system is minimized by numerically integrating the Langevin equation using a Crank−Nicolson scheme. Zero potential fields and homogeneous density distributions form the starting configuration for the integration. The integration is carried out as long as the density fields change significantly. Using an order parameter P, defined below, the evolution of the density fields is monitored.

$$P \equiv \frac{v^2}{V} \sum_I \int_{\vec{r}} (\rho_I^2(\vec{r}) - \bar{\rho}_I^2) \mathrm{d}\vec{r} \tag{5}$$

At $t = 0$ P equals zero. P levels off when the system has reached its equilibrium state or becomes trapped in a local minimum. It has to be remarked that P is only a measure for the grade of demixing of unlike beads and is by definition insensitive to morphological transitions, which do not involve significant changes in the grade of demixing. Therefore, we have used P together with a direct evaluation of the density fields.

It is important to notice that even when no dynamics is observed in the density fields, it is still possible that the system has not reached a global or local equilibrium. This could be the case when the time scales of the dynamics are beyond the time scale covered by our simulations.

D. Parameters. The simulations are done on a cubic grid of dimensions $X \times Y \times Z = 32 \times 32 \times W$ ($W = H + 2$ and H is the width of the slit), with a lattice spacing h. Periodic boundaries are used in all directions. The slit surfaces are placed on the top and bottom face of the box.

In our calculations, we use the same polymer model (A_3B_6) as in our previous study.[5] An optimal value for the bond length a and grid base h is used.[15] The energetic interaction between equivalent beads is set to zero ($\epsilon^\circ_{AA} = \epsilon^\circ_{BB} = 0$) and A−B interaction is chosen to be repulsive ($\epsilon^\circ_{AB}/vkT = \chi = 2$). The compressibility is set to $\kappa_H/kT = 6$. This polymer model models the statistic behavior of a SB (polystyrene−polybutadiene) block copolymer with a $M_w \approx 35\,000$ g/mol at $T \approx 413$ K. This temperature is close to the temperature used in experiments to anneal thin films of SBS to obtain the equilibrium structure.[16] The bulk morphology of the A_3B_6 model at this temperature consists of A-rich cylinders embedded in a B-rich matrix, with a bulk domain−domain distance $D \approx 7$ (grid points).

In this study we vary the slit width H and the effective interaction, $\xi \equiv (\epsilon^\circ_{AM} - \epsilon^\circ_{BM})/vkT$.

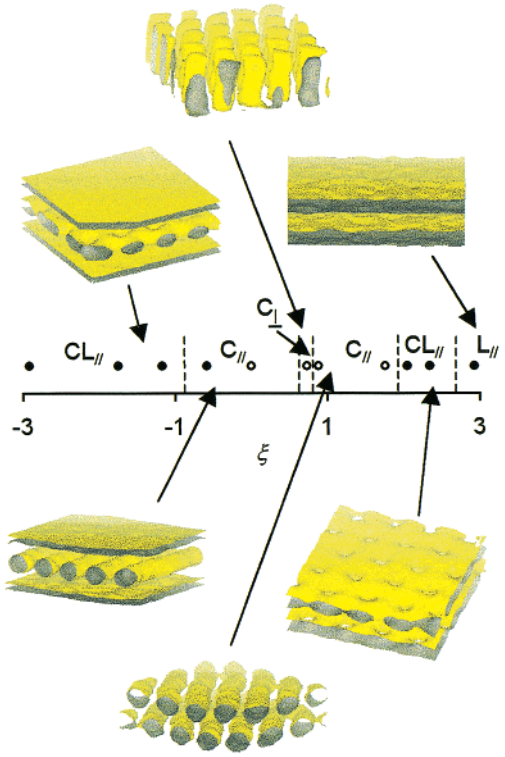

Figure 1. Influence of the surface−polymer interactions $\xi \equiv (\epsilon^\circ_{AM} - \epsilon^\circ_{BM})/vkT$ on the morphology of the A-rich domains in slit with $H = 12$ (the dashed lines mark the transition points). Different morphologies are visualized with the help of the isodensity surfaces of the A-beads ($\phi = 0.33$). The solid dots refer to the calculations done in this study. The open circles represent data from our previous calculations.[5]

III. Results and Discussion

A. Surface Fields. First of all, we want to get an idea how surface fields affect the microstructure of a thin film. We have systematically increased ξ from −3 (preferential wetting by the A-blocks) up to 3 (preferential wetting by the B-blocks) for a system confined in a slit with width ($H = 12$). We have chosen this value because $H = 12$ has proven to be the equilibrium thickness of a free A_3B_6 film.[5] Various morphologies are predicted: $C_\perp$ (perpendicular cylinders), $C_{||}$ (parallel cylinders), $CL_{||}$ (cartenoid−lamellae), and $L_{||}$ (lamellae). The isodensity surfaces of the A beads ($\phi = 0.33$) of the different morphologies are shown in Figure 1. We have discussed $C_\perp \rightarrow C_{||}$ transitions in great detail in our previous study.[5] The two interesting points of our present calculations are the prediction of morphology transitions driven by the surface fields ($C_{||} \rightarrow CL_{||}$ and $CL_{||} \rightarrow L_{||}$) and the asymmetry in the phase behavior with respect to ξ (no $L_{||}$ phase is found for the case where the A-blocks preferentially wet the surfaces). The discussion of this second feature will be postponed to the following section.

The coupling between the surface fields and the density profiles induces transitions from cylindrical to noncylindrical structures. In the simulations, the surface fields do not vary in lateral direction. Therefore, they tend to suppress bead density variations parallel to the slit surfaces and drive the system toward noncylindrical structures: $CL_{||}$ and $L_{||}$ in our case. It has already been predicted with a quasi 2D WSL analysis that lamellar morphologies could be stable in films with strong preferential wetting of the surfaces by one of the polymer blocks.[3] The interesting difference between our results and the 2D WSL calculations is the $CL_{||}$ phase. Whereas the WSL approach predicts a direct transition from $C_{||} \rightarrow L_{||}$ we find two separate transitions: $C_{||} \rightarrow CL_{||}$ and $CL_{||} \rightarrow L_{||}$. That cartenoid−lamellae phases have not been predicted by the WSL calculations is due to the assumption that the system is homogeneous in one direction. The $CL_{||}$ phase cannot be described with such a quasi-2D model.

There is some experimental evidence for the stability of the $CL_{||}$ phase in a thin film system.[7,8] However, for bulk systems, the $CL_{||}$ phase was found to be a metastable state with a very long lifetime.[17] This cast some doubts on our findings. We have performed two "experiments" to investigate the stability of the $CL_{||}$ phase. That the $CL_{||}$ phase is more stable than the $L_{||}$ phase can be seen in Figure 2. In this figure, we have plotted the isodensity profiles at various time steps at $\xi \sim 2.3$. Initially lamellae are formed. After a certain amount of time holes nucleate in this lamellae and the $CL_{||}$ phase develops. That the $CL_{||}$ phase is more stable then the $C_{||}$ phase at $\xi \sim 2.3$ has been proven by a simulation in which we equilibrated a system at $\xi = 1.75$ (resulting in $C_{||}$) for 4000 time steps. After this equilibration, we changed ξ to 2.3. In Figure 3, we have plotted the isodensity profiles at different time steps. Note that $y = 4000$ is just before the moment that ξ is changed to its final value. Clearly, the $CL_{||}$ phase develops rather quickly. We can conclude that the cartenoid−lamellae can be stable in a slit or film.

B. Confinement. In this section, we study the influence of the slit width (film thickness) on the

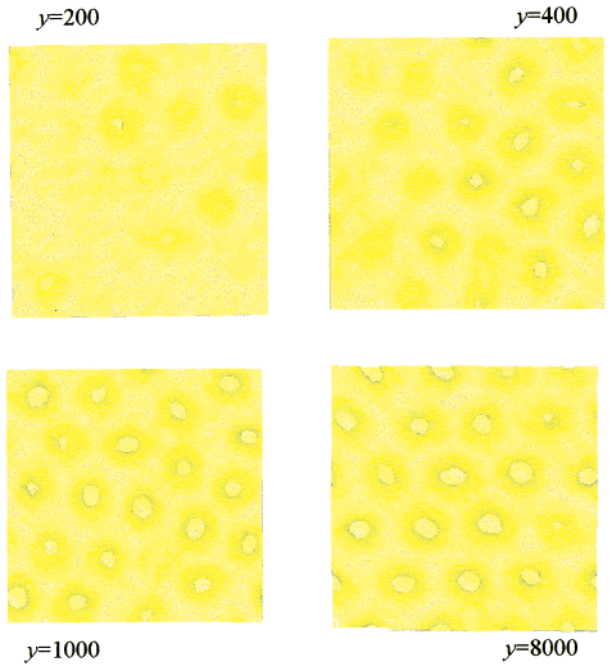

Figure 2. Top view of the isodensity surfaces of the A-beads ($\phi = 0.33$) at different times ($\xi = 2.34$, $H = 12$).

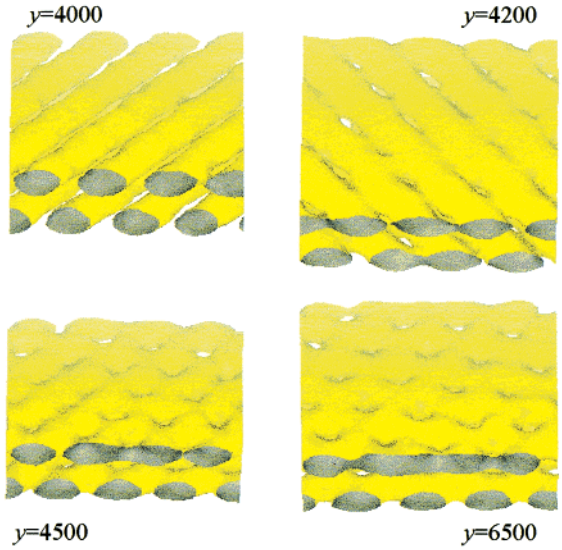

Figure 3. Isodensity surfaces of the A-beads ($\phi = 0.33$) at different times ($\xi = 2.34$, $H = 12$). We switched from ξ from 1.75 to 2.34 at $y = 4000$.

noncylindrical morphologies. We have done various simulations for a limited range of slit widths $H = 9-15$. From our previous study[5] we know that the values $H = 9$ and 15 are the boundary values for a system with a constant number of layers, e.g., n. At $H = 9$ and 15, perpendicular cylinders are stable, and for $H < 9$ and $H > 15$, we have a different number of layers ($n - 1$ and $n + 1$). We have constructed a phase diagram; see Figure 4. The solid dots are the calculated points, and the open circles are data points from our previous study.[5] The lines represent the proposed phase boundaries (dashed lines are used in the case of large uncertainties). We have to remark that an exact determination of the morphology is not always as simple as that suggested by the phase diagram, especially for low values of H at $\xi \sim 3$ (see i.e., Figure 5).

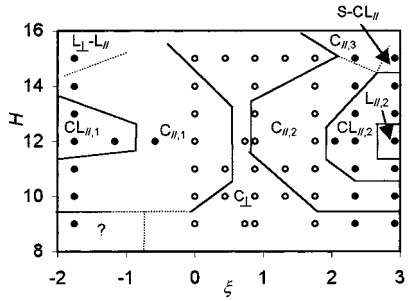

Figure 4. Phase diagram of an A_3B_6 melt confined in a slit (film). The solid dots refer to the calculations done in this study. The open circles represent data from our previous calculations.[5] The solid lines mark the proposed phase boundaries. Dashed lines are used in the case of large uncertainties. The symbols refer to the various morphologies: perpendicular oriented cylinders ($C_\perp$), parallel oriented cylinders ($C_{||}$), carteinoid−lamellae ($CL_{||}$), lamellae ($L_{||}$), mixed spheres and cartenoid−lamellae ($S - CL_{||}$), and mixed parallel and perpendicular lamellae ($L_\perp - L_{||}$). The question mark refers to a system with a low degree of mixing. The numbers added to the symbols refer to the number of layers of A-rich domains excluding the boundary layer.

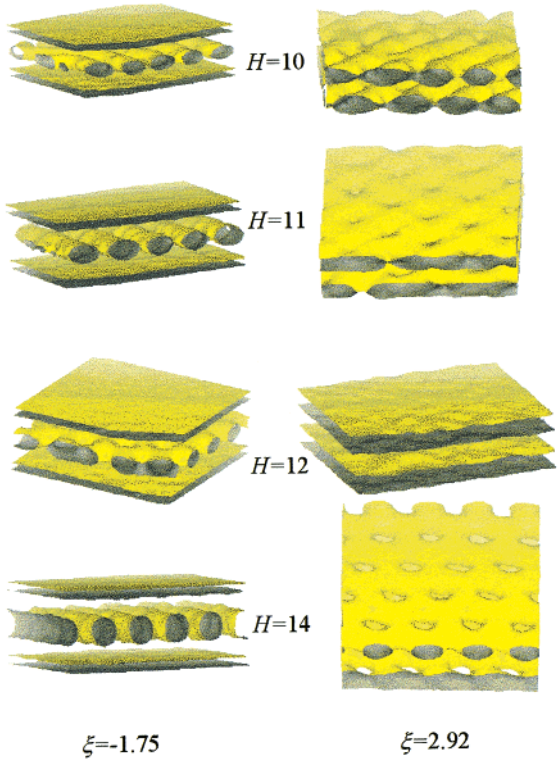

Figure 5. Isodensity surfaces of the A-beads ($\phi = 0.33$) for different slit widths at $\xi = +2.92$ (right) and -1.75 (left).

The phase diagram has a number of interesting features. The first interesting feature of the phase diagram is its asymmetry. In the previous section, we already touched on this point (see Figure 1). This asymmetry indicates that it is easier to stabilize noncylindrical structures with surfaces preferentially wet by the longest block (B) then with surfaces preferentially wet by the smallest block (A) of the polymer. We think that in the A-wet case the number of A-blocks, available for the A-rich layer in the center of the slit, is to small to form a perfect lamella. Too many A-blocks are drawn to the surfaces due to the strong attraction by these surfaces.

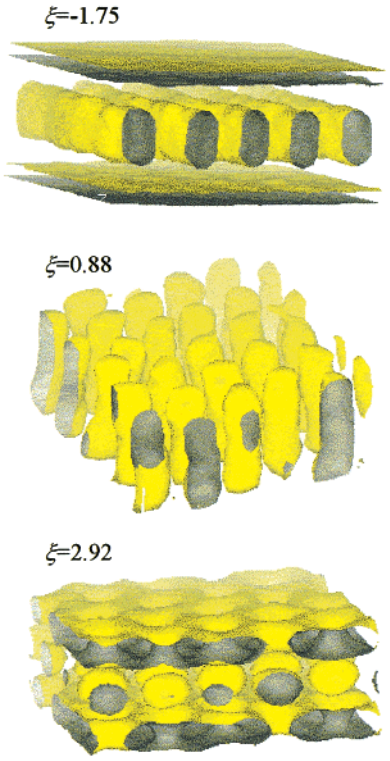

Figure 6. Isodensity surfaces of the A-beads ($\phi = 0.33$) in the $n \leftrightarrow n + 1$ transition region at $H = 15$.

The second point of interest is the sequence of phases the system goes through when the slit width varies. To visualize this we have plotted the isodensity surfaces of the A beads ($\phi = 0.33$) (Figure 5) for various values of H at $\xi = -1.75$ (left) and 2.92 (right). In our previous study,[5] we only found the $C_{||} \rightarrow C_{\perp}$ transition when we varied H from 10 to 15. Here, we find two to four transitions for the same range of H, depending on the value of ξ. There seems to be a general rule for the evolution of the morphology with H. The most homogeneous structure (in the $X-Y$ plane) is always formed at $H = 12$, which is halfway into the n-layer domain. Close to the $n - 1 \leftrightarrow n$ ($H = 9$) and $n \leftrightarrow n + 1$ ($H = 15$) transition regions, the surfaces are less capable in suppressing density variations in the direction parallel to the surfaces.

This complex behavior cannot be explained without a detailed study of the H-dependence of the free energy for every structure separately, which is beyond the scope of this study. At least we can conclude that the microstructure of the system is very sensitive to the slit width when there is a strong preferential attraction between the surfaces and one of the polymer blocks.

The third interesting feature of Figure 4 is the phase behavior at $H = 15$. We have plotted the isodensity surfaces ($\phi = 0.33$) for various values of ξ in Figure 6. The existence of the $C_{\perp}$ structure at $H = 15$ has already been predicted and explained in our previous study.[5] Here, we see that the $C_{\perp}$ phase becomes unstable below and above a certain value of ξ. For $\xi = -1.75$ a mixed lamellar morphology is formed, $L_{\perp} - L_{||}$. Perpendicular oriented A-rich lamellae are formed, which do not extend to the top surfaces. These perpendicular lamellae are in fact fused cylinders. For $\xi = 2.92$ a totally different structure is formed, $S - CL_{||}$. Three A-rich layers are formed. The top and bottom layers are perforated lamellae, and in the center of the system, a layer of hexagonal packed spheres is formed. The spheres are located at the same $X-Y$ positions as the holes in the lamellae. The spheres can be regarded as the smallest possible perpendicular cylinders. The origin of a mixed morphology of perpendicular cylinders and cartenoid lamellae will be discussed in section III.C.

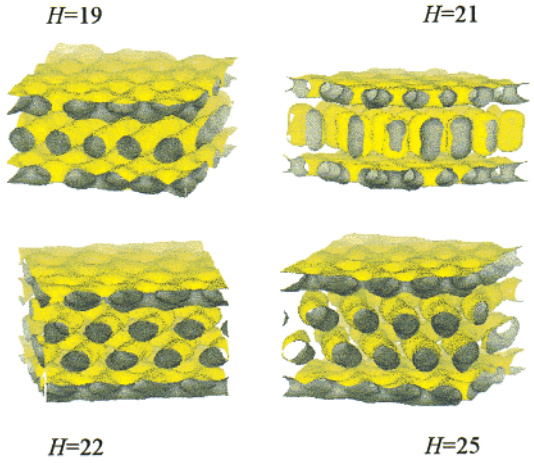

Figure 7. Isodensity surfaces of the A-beads ($\phi = 0.33$) for various slit widths at $\xi = 2.92$.

At the end of this section we have to remark that there is little experimental data available to validate the simulations results. However, our results show at least that the behavior of the films of asymmetric diblock copolymers with very selective surfaces is still a challenging subject with many open questions.

C. Range of Influence of the Surface Fields. Till now we only investigated very thin systems: slits with a width H of the order of one or two times the domain−domain distance in a bulk material D (∼7). It was shown that in these systems the overall morphology is strongly influenced by the presence of surfaces. In this section, we want to investigate how far from the surfaces the morphology of the polymer melt is influenced. To do this, we have systematically varied H for the case of strong preferential wetting by the B-blocks ($\xi = 2.34$ and 2.92; $H = 16, 17, \ldots, 25$). We have plotted the isodensity surfaces of the A-blocks (Figure 7) for various values of H at $\xi = 2.92$.

In all calculations, we observed mixed morphologies. The A-rich domains close to the surface adopted noncylindrical morphologies. In the center of the slit the A-blocks always segregated into cylindrical domains as in a bulk system. This suggests that in this particular system the influence of a surface is only felt in a layer (with thickness of order D) adjacent to this surface. This can be understood as follows. The range of influence is comparable to the correlation length of the system. And in our case the correlation length is comparable with D, because we are far from the order−disorder transition in the bulk.

An interesting observation to be considered here is that the behavior of the domains far from the surfaces is closely related to their behavior in systems with a lower value of ξ as has been studied previously (∼1.75).[5] For nearly all values of H, the inner part has a $C_{||}$ structure. Only at $H = 21$ are perpendicular oriented cylinders $C_{\perp}$ found. In Figure 8, we have drawn schematic picture to explain this phenomenon. When we regard the top and bottom layers of the system as a part of the slit walls, then we are in fact studying a block copolymer melt confined between two surfaces with a

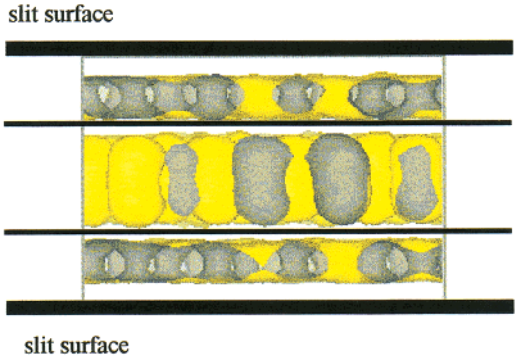

Figure 8. Side view of the isodensity surface of the A-beads ($\phi = 0.33$) ($\xi = 2.92$, $H = 21$). The solid lines are placed as guide for the eye and mark the inner part of the system. This part of the system behaves as a system with $\xi \sim 1.75$.

strong B-character. Following this line of thought, we may consider the phase diagram for the reduced system, the system minus the top and bottom layer and effective interaction equal to the A−B interaction. For this type of systems we can easily show that $\xi \approx \epsilon^{\circ}_{AB}/vkT = \chi$ and thus $\xi \sim 2$, which is indeed close to 1.75.

Conclusions

In this paper, we have discussed the influence of polymer−surface interactions on the morphology of an asymmetric diblock copolymer film. We have focused on block copolymers that form cylinders in the bulk (A_nB_m, 33% A). We were especially interested in transitions to noncylindrical structures induced by surface fields. A DDFT model was used to find equilibrium structures. The effective surface−polymer interaction ξ (the difference between the A−surface and B−surface interactions) and the film thickness H have been varied systematically.

We have found that noncylindrical structures can become stable when the effective interaction is high and the surfaces are preferentially wet by one of the blocks. Parallel oriented cartenoid lamellae ($CL_{||}$) and lamellae ($L_{||}$) were formed. Surface fields do not induce a direct transition from parallel oriented cylinders ($C_{||}$) toward lamellae. When the B−surface interaction was increased, first (ξ increasing from 1.75 to ~3) a $C_{||} \rightarrow CL_{||}$ and later a $CL_{||} \rightarrow L_{||}$ transition occurred.

We have predicted a detailed phase diagram for a limited range of film thicknesses ($\Delta H \approx D$, D is the domain−domain distance in the bulk). It was found that strong surface fields stabilize a variety of phases, which are unstable at smaller effective interactions. The higher the interaction of the surfaces with one of the polymer blocks the more sensitive is the microstructure to variations in H.

The phase diagram also made clear that the phase behavior is asymmetric: surface fields, promoting A-wetting ($\xi < 2$), are less capable in stabilizing noncylindrical structures when compared to surface fields, promoting B-wetting ($\xi > 3$). We did not find a $L_{||}$ phase for $\xi \ll 0$. We think that the number of A-blocks in the center of a film is to low to form a stable lamella when the A-blocks wet the surfaces.

Calculations on thicker films with B-wet surfaces have shown that the range of influence of the surface fields is of order D. Therefore, close to the surface noncylindrical structures are stabilized. Far away from the surface ($>D$) cylinders are formed. The orientation of these cylinders (parallel or perpendicular) varied with the film thickness in a way closely related with the behavior of a film with a lower effective interaction. The inner part of the film can be thought of as a polymeric melt confined between two surfaces with strong B-character and therefore a different and fixed effective interaction, namely the bead−bead interaction.

Finally, we have to remark that the main experimental focus has been on symmetric diblock copolymers. Therefore, our results are challenging for both theoreticians and experimentalists, because they are so different from symmetric diblock case. By simulations we have shown that the microstructure of a thin film of asymmetric diblock copolymers is extremely sensitive to the film thickness and surface−polymer interaction. These findings offer an interesting starting point and important apriori knowledge, for a renewed effort in both experimental and theoretical investigations.

Acknowledgment. Part of this study has been carried out at the Shell Research and Technology Centre in Amsterdam (SRTCA). We thank Hans Fraaije, Andrei Zvelindovsky (Leiden Institute of Chemistry), and Wouter Koot (SRTCA) for useful discussions. Support for this project was provided by the MesoDyn project ESPRIT, No. EP22685, of the European Community.

References and Notes

(1) Matsen, M. W. *Curr. Opin. Colloid Interface Sci.* **1998**, *3*, 40.
(2) Binder, K. *Adv. Polym. Sci.* **1999**, *138*, 1.
(3) Turner, M. S.; Rubinstein, M.; Marques, C. M. *Macromolecules* **1994**, *27*, 4986.
(4) Suh, K. Y.; Kim, Y. S.; Lee, H. H. *J. Chem. Phys.* **1998**, *108*, 1253.
(5) Huinink, H. P.; Brokken-Zijp, J. C. M.; van Dijk, M.; Sevink, G. J. A. *J. Chem. Phys.* **2000**, *112*, 2452.
(6) Liu, Y.; Zhao, W.; Zheng, X.; King, A.; Singh, A.; Rafailovich, M. H.; Sokolov, J.; Dai, K. H.; Kramer, E. J.; Schwarz, S. A.; Gebizlioglu, O.; Sinha, S. K. *Macromolecules* **1994**, *27*, 4000.
(7) Radzilowski, L. H.; Carvalho, B. L.; Thomas, E. L. *J. Polym. Sci., Polym. Phys.* **1996**, *34*, 3081.
(8) Harrison, C.; Park, M.; Chaikin, P. M.; Register, R. A.; Adamson, D. H.; Yao, N. *Macromolecules* **1998**, *31*, 2185.
(9) Fraaije, J. G. E. M.; van Vlimmeren, B. A. C.; Maurits, N. M.; Postma, M.; Evers, O. A.; Hoffmann, C.; Altevogt, P.; Goldbeck-Wood, G. *J. Chem. Phys.* **1997**, *106*, 4260.
(10) van Vlimmeren, B. A. C.; Maurits, N. M.; Zvelindovsky, A.; Sevink, G. J. A.; Fraaije, J. G. E. M. *Macromolecules* **1999**, *32*, 646.
(11) Zvelindovsky, A.; Sevink, G. J. A.; van Vlimmeren, B. A. C.; Maurits, N. M.; Fraaije, J. G. E. M. *Phys. Rev. E* **1998**, *57*, R4879.
(12) Sevink, G. J. A.; Zvelindovsky, A.; van Vlimmeren, B. A. C.; Maurits, N. M.; Fraaije, J. G. E. M. *J. Chem. Phys.* **1999**, *110*, 2250.
(13) Sevink, G. J. A.; Fraaije, J. G. E. M.; Huinink, H. P. *submitted to Macromolecules* 2000.
(14) Maurits, N. M.; van Vlimmeren, B. A. C.; Fraaije, J. G. E. M. *Phys. Rev. E* **1997**, *56*, 816.
(15) Maurits, N. M.; Altevogt, P.; Evers, O. A.; Fraaije, J. G. E. M. *Comput. Theor. Polym. Sci.* **1996**, *6*, 1.
(16) van Dijk, M. A.; van den Berg, R. *Macromolecules* **1995**, *28*, 6773.
(17) Frederickson, G. H.; Bates, F. S. *Annu. Rev. Mater. Sci.* **1996**, *26*, 501.

MA000015H